

1 **Reduced frontal white matter microstructure in healthy older adults**
2 **with low tactile recognition performance**

3 Focko L. Higgen^{1#*}, Hanna Braaß^{1#} MD, Robert Schulz¹ MD, Gui Xue² PhD, Christian Gerloff¹
4 MD

5 ¹ Department of Neurology, University Medical Center Hamburg-Eppendorf, 20246 Hamburg,
6 Germany

7 ² State Key Laboratory of Cognitive Neuroscience and Learning, Beijing Normal University,
8 Beijing, China, 100875

9 # Both authors contributed equally

10

11 *** Corresponding author:**

12 Focko L. Higgen

13 University Medical Center Hamburg-Eppendorf

14 Martinstraße 52, 20246 Hamburg, Germany

15 Phone: +49-40-7410-55573

16 Facsimile: +49-40-7410-57391

17 Email: f.higgen@uke.de

18

19 **Running title:** DTI, aging and tactile recognition

20

21 **Abstract**

22 Aging leads to a reduction of connectivity in large-scale structural brain networks. Sensory
23 processing and other cognitive processes rely on information flow between distant brain areas.
24 However, data linking age-related structural brain alterations to cognitive functioning, especially
25 sensory processing, is sparse.

26
27 Aiming to determine group differences in sensory processing between older and younger
28 participants, we implemented a complex tactile recognition task and investigated to what extent
29 changes in microstructural white matter integrity of large-scale brain networks might reflect
30 success in task performance. Structural brain integrity was accessed by means of diffusion-
31 weighted imaging and fractional anisotropy.

32
33 The data revealed that poor performance in complex tactile recognition in older, neurologically
34 healthy individuals is related to decreased structural integrity pronounced in the anterior corpus
35 callosum. This region was strongly connected to the prefrontal cortex. Our data suggests decreased
36 fractional anisotropy in the anterior corpus callosum as a surrogate marker for progressed brain
37 aging, leading to disturbances in networks relevant for higher-order cognitive processing. Complex
38 tactile recognition might be a sensitive marker for identifying these starting cognitive impairments
39 in older adults.

40

41 **Keywords:** aging, corpus callosum, PFC, sensory, tbss, tractography

42 **1 Introduction**

43 Older adults face the challenges of aging-related cognitive impairments. As some of the key
44 features, these comprise processing of sensory stimuli, decision making and subsequent actions
45 (Anguera and Gazzaley, 2012; Gazzaley et al., 2005; Guerreiro et al., 2014; Zheng et al., 2018).
46 Age-related sensory impairments affect all senses, e.g. visual acuity and auditory and tactile
47 thresholds, and have great impact on the independency and the activities of daily living (Freiherr
48 et al., 2013). Therefore, the investigation of sensory processing might give valuable insight into
49 mechanisms of aging.

50

51 The underlying reasons for age-related deficits are manifold. Going clearly beyond the importance
52 of decreases of function of peripheral sensory organs, the brain undergoes continuous
53 modifications throughout the life span (Gazzaley et al., 2005; Heise et al., 2014, 2013). These age-
54 related alterations in central processing can be analyzed on different spatial scales. On a micro-
55 scale, there are changes of cellular properties, morphology, transmitter levels and neural plasticity
56 (Hong and Rebec, 2012; Kumar and Foster, 2007). On a meso-scale, these changes lead to
57 alterations of functional neuronal activations (Heise et al., 2014, 2013; Quandt et al., 2016; Sailer
58 et al., 2000) and consequently to large-scale alterations of brain structure and function on the
59 network-level (Babaeeghazvini et al., 2018; Heuninckx et al., 2008; Michely et al., 2018; Raz and
60 Rodrigue, 2006; Schulz et al., 2014).

61

62 Sensory processing relies on local brain activation and interregional information flow between
63 primary and higher order sensory areas. Especially processing of complex stimuli needs an
64 interplay between different brain regions and therefore requires proper structural integrity of large-

65 scale networks (Göschl et al., 2015; Hipp et al., 2011). For tactile recognition, there is an
66 interaction of bottom-up sensory flow with top-down control (Adhikari et al., 2014; Sathian, 2016;
67 Stilla et al., 2007). Bottom-up tactile inputs are primarily processed in the primary somatosensory
68 cortex (S1) and then segregated into different pathways for different object properties. Relevant
69 cortical areas of this distributed network include the parietal operculum (SII), the posterior parietal
70 cortices, the intraparietal sulcus, the temporo-parietal junction and the limbic areas (Mauguière et
71 al., 1997; Sathian, 2016; Van Boven et al., 2005). Concurrently, tactile processing is mediated by
72 higher cognitive functioning such as top-down attentional control and visuo-spatial working
73 memory. These functions are executed via inputs from the prefrontal cortices (PFC), comprising
74 for example the dorsolateral prefrontal cortex (DFPLC) and the ventrolateral prefrontal cortex
75 (VLPFC) (Adhikari et al., 2014; Deibert et al., 1999; Reed et al., 2004; Sathian, 2016).

76 Taken together, alterations in both, networks of bottom-up sensory flow and networks of top-down
77 modulation, could lead to disturbances in sensory processing.

78

79 There have been multiple neuroimaging studies accessing large-scale brain network integrity in
80 relation to aging processes. A measurement widely accepted to describe brain network integrity is
81 fractional anisotropy (FA), a parameter derived from diffusion-weighted brain imaging. Within
82 the limitations of fiber-tracking, FA is commonly referred to as a neuroimaging index of micro-
83 structural white matter integrity (Hugenschmidt et al., 2008; Kochunov et al., 2012; Schulz et al.,
84 2015). In the following we will use the term accordingly.

85 A common finding is a wide-spread reduction of FA with increasing age (Abe et al., 2002;
86 Carmichael and Lockhart, 2012; Kochunov et al., 2007; Madden et al., 2012, 2009; Malloy et al.,
87 2007; Minati et al., 2007; Moseley, 2002; Salat, 2011; Sullivan and Pfefferbaum, 2007, 2006;

88 Wozniak and Lim, 2006). This so called ‘cortical disconnection’ is thought to contribute to age-
89 related cognitive decline (Bennett and Madden, 2014). Domains that have been shown to be
90 affected by the decrease of micro-structural white matter integrity mainly comprise higher
91 cognitive functioning such as executive functioning, processing speed and memory (for review see
92 Bennett and Madden, 2014). So far, data linking these age-related structural alterations with basic
93 sensory processing, is sparse (Chalavi et al., 2018; Damoiseaux, 2017).

94

95 Aiming to determine group differences in sensory processing between older and younger
96 participants, we implemented a complex tactile recognition task. All participants underwent
97 structural brain imaging including diffusion weighted imaging to characterize global white-matter
98 microstructure. We hypothesize that inter-subject variability in microstructure of large-scale
99 structural brain networks is related to variable success in complex sensory processing at the
100 behavioral level.

101 **2 Material and Methods**

102 **2.1 Participants**

103 37 and 22 younger volunteers were screened for the study. 6 older volunteers did not meet the
104 inclusion criteria during initial assessment. 2 older and 2 younger participants dropped out because
105 of personal or technical problems. During task performance, 10 older participants did not meet the
106 predefined accuracy targets (as described below) and older participants were regrouped into O-LP
107 (older-low-performers) and O-HP (older-high-performers). Thus, 10 O-LP (5 female, mean age
108 74.1, range 68-82), 19 O-HP (11 female, mean age 71.9, range 65-79) and 20 younger participants
109 (= Young, Y; 11 female, mean age 24.1, range 20-28) entered in the final analyses.

110 All participants were right handed according to the Edinburgh handedness inventory (Oldfield,
111 1971), had normal or corrected to normal vision, no history or symptoms of neuro-psychiatric
112 disorders (MMSE \geq 28, DemTect \geq 13) and no history of centrally acting drug intake. All
113 participants received monetary compensation.

114 **2.2 Ethics statement**

115 The study was conducted in accordance with the Declaration of Helsinki and was approved by the
116 local ethics committee of the Medical Association of Hamburg (PV5085). All participants gave
117 written informed consent.

118 **2.3 Assessment**

119 Prior to inclusion, each participant underwent an assessment procedure. Assessment consisted of
120 a neurological examination, the Mini-Mental State (MMSE, cut-off \geq 28; Folstein et al., 1975) and
121 the DemTect (cut-off \geq 13; Kalbe et al., 2004) to rule out symptoms of neuro-psychiatric disorders.
122 Furthermore, a 2-point-discrimination test (cut-off $>$ 3mm; Crosby and Dellon, 1989; Dellon et
123 al., 1995) and a test of the mechanical detection threshold (MDT, v. Frey Filaments, OptiHair2-

124 Set, Marstock Nervtest, Germany, cut-off > 0.75mN; Fruhstorfer et al., 2001; Rolke et al., 2006)
125 were conducted to ensure intact peripheral somatosensation. We also assessed subjectively
126 experienced attention deficits with a standardized questionnaire (FEDA). The FEDA is divided
127 into sub-sections A, B and C, where A asks for distractibility and slowing up in mental processes,
128 B for fatigue and slowing up in practical activities and C for reduction of energy (Zimmerman and
129 Lahav, 2012).

130 **2.4 Task design**

131 The experiment took place in a light attenuated chamber. We chose experimental procedure,
132 stimulus configuration, and stimulation parameters based on pilot data showing accuracy of tactile
133 pattern recognition to be very different between older and younger participants.

134 For tactile stimulation, the participants' right hand was resting on a custom-made board containing
135 a Braille stimulator (QuaeroSys Medical Devices, Schotten, Germany), with the fingertip of the
136 right index finger placed above the stimulating unit (see suppl. figure 1). The Braille stimulator
137 consists of eight pins arranged in a four-by-two matrix, each 1mm in diameter with a spacing of
138 2.5mm. Each pin is controllable independently. Pins can be elevated (maximum amplitude 1.5mm)
139 for any period to form different patterns. At the end of each pattern presentation, all pins return to
140 baseline. The tactile recognition task consisted of steps of increasing complexity. At the beginning
141 of each step participants read the task instructions on a computer screen positioned in front of
142 them. The stimuli consisted of different sets of four geometric patterns, each of them formed by
143 four dots (figure 1a). The experiment began with a very simple set of four familiarization patterns
144 (step 1, figure 1a, b) at maximum pin amplitude and a stimulation time of 800ms to get the
145 participants acquainted with the tactile stimulation.

146 Each trial started with a central white fixation point appearing on a noisy background. This fixation
147 point remained visible throughout each single trial. The tactile pattern presentation started 1500ms
148 after appearance of the fixation point with a stimulus chosen pseudo-randomly from the stimulus
149 set. After the tactile presentation, there was a waiting interval of 1200ms. Then, the central fixation
150 point turned into a question mark and participants indicated which of the four patterns had been
151 presented. Participants responded via button press with the fingers two to five of the left hand.
152 After each trial participants received visual feedback (1000ms) whether response was correct
153 (green '+') or incorrect (red '-') (figure 1c).

154 After a minimum of five familiarization blocks, each one consisting of 16 trials, and an accuracy
155 of at least 75% in three of five consecutive blocks, participants could proceed to the next step. If
156 participants did not reach the target accuracy within 15 blocks, they were excluded from further
157 participation.

158 In the next step of the recognition task, the stimulus set consisted of the four target patterns (step
159 2, figure 1a, b). To train participants in the recognition of the target patterns, stimulation occurred
160 at maximum amplitude and again with a long stimulation time of 800ms. Trial timing, blocks and
161 accuracy targets were always as described above. If again participants were able to recognize
162 patterns with the previously defined accuracy, in the final step of the recognition task stimulation
163 time of the target patterns was 500ms (step 3, figure 1a, b). Participants who were able to recognize
164 these patterns with the targeted accuracy were categorized as "high-performers". Participants not
165 reaching this level were labeled "low-performers". We grouped all participants not reaching the
166 predefined accuracy target at one of the steps of the tactile recognition task together, as they all
167 did not show any deficits in the initial assessment, but a clear performance difference in tactile
168 recognition compared to the younger participants and the older "high-performers". In all these

169 participants alterations in microstructure of large-scale structural brain networks might be the
170 reason for poor performance, according to our initial hypotheses.

171

172 - Figure 1 here -

173

174 **2.5 Brain Imaging**

175 A 3 Tesla MRI system (Magnetom Skyra, Siemens Healthcare, Erlangen, Germany) and a 32-
176 channel head coil acquired diffusion-weighted and high-resolution T1-weighted structural images.

177 For the diffusion-weighted sequence, a spin-echo, echo-planar imaging (EPI) sequence was
178 applied with the following parameters: TE = 82ms, TR = 10000ms, flip angle = 90°, matrix size =

179 104 × 128 matrices, FOV = 208 × 256 mm², voxel resolution = 2.0 × 2.0 × 2.0 mm³, partial Fourier

180 factor = 0.75, 75 contiguous transversal slices, one image with b = 0 s/mm², 64 images with b =

181 1500s/mm² (64 non-collinear directions). For the T1-weighted sequence, a 3-dimensional

182 magnetization-prepared rapid gradient echo (3D-MPRAGE) sequence was used with the following

183 parameters: TR = 2500ms, TE = 2.12ms, TI = 1100ms, flip angle 9°, 256 coronal slices with a

184 voxel size of 0.83 × 0.94 × 0.83mm³, FOV = 240 mm.

185 **2.6 Image processing**

186 The processing and analysis of MRI data were carried out using FMRIB Software Library (FSL)

187 software 5.0.2.2 (Analysis Group, FMRIB, Oxford, UK Oxford Centre for Functional Magnetic

188 Resonance Imaging of the Brain Software Library, <https://fsl.fmrib.ox.ac.uk/fsl/fslwiki/FSL>)

189 (Smith et al., 2004). First, the eddy current distortion and simple head motion of raw diffusion data

190 were corrected, using Eddy current correction from the FMRIB's Diffusion Toolbox (FDT) 3.0.

191 Then, the Brain Extraction Tool (BET) v2.1 of FSL was used for brain extraction (Smith, 2002).

192 FA images were created by fitting a tensor model in each voxel to the raw diffusion data using
193 FDT, additionally the eigenvalue images for L1, L2 and L3 were created in the same way.

194 **2.7 Tract-Based Spatial Statistics (TBSS)**

195 Voxelwise statistical analysis of the created FA data was carried out using TBSS (Tract-Based
196 Spatial Statistics) (Smith et al., 2006). All subjects' FA data were nonlinearly registered to the
197 FMRIB58-FA standard-space template (FMRIB Centre University of Oxford, Department of
198 Clinical Neurology, John Radcliffe Hospital Headington, Oxford,
199 UK; https://fsl.fmrib.ox.ac.uk/fsl/fslwiki/FMRIB58_FA) and aligned to the Montreal
200 Neurological Institute (MNI) space using the nonlinear registration tool FNIRT (Andersson et al.,
201 2007a, 2007b) as part of TBSS, which uses a b-spline representation of the registration warp field
202 (Rueckert et al., 1999). Next, the mean FA image was created and thinned to create a mean FA
203 skeleton, which represents the centers of all tracts common to the group. Each subject's aligned
204 FA data was then projected onto this skeleton and the resulting data fed into voxelwise cross-
205 subject statistics. The permutation-based non-parametric inferences within the framework of the
206 general linear model were performed to investigate the differences between the groups Young
207 versus older-high-performers (Y vs. O-HP), young versus older-low-performers (Y vs. O-LP) [1 -
208 1; -1 1] and older-high-performers (O-HP) versus older-low-performers (O-LP) [1 -1; -1 1] using
209 randomise (<https://fsl.fmrib.ox.ac.uk/fsl/fslwiki/Randomise>). For corrected results the threshold-
210 free cluster enhancement with the family-wise error (FWE) correction for multiple comparisons
211 corrections ($P < 0.05$, FWE corrected, 5000 permutations) was used.

212 The brain regions in which the analysis showed significantly different FA-values between the two
213 groups were thresholded at P-value < 0.05 . In the next step we used these resulting brain regions
214 to create individual masks for each subject. To create these individual masks the resulting brain

215 regions in the anterior corpus callosum, were first binarized and in a second step back-transformed
216 to the individual diffusion space. The individual binary masks were then multiplied with the
217 individual FA-maps. We calculated the mean FA in the resulting image for each participant and
218 used the mean FA-values for further statistical calculations. Mean FA values measured in a second
219 region in the splenium corpus callosum in all older participants served as a control. The region in
220 the splenium was manually defined on the MNI152_T1_1mm image in the Splenium corpus
221 callosum, symmetrical to the midline of the brain (volume: 229 voxel). Additionally, axial (AD)
222 and radial diffusivities (RD) in the anterior corpus callosum were computed in the same way.

223 **2.8 Probabilistic Tractography**

224 After preprocessing the DWI-data with eddycorrect and BET as described above FSL's bedpostx
225 was used to estimate the distribution of diffusion parameters in each voxel, modelling crossing
226 fibers using Markov Chain Monte Carlo sampling (Behrens et al., 2007). Probabilistic tractography
227 was used to reconstruct the tracts with the region defined in the anterior corpus callosum (as
228 mentioned above) as seed mask (5000 streamlines sent from each voxel in the individual seed
229 masks, curvature threshold 0.2, steplength 0.5mm). In each participant, tracts starting from the
230 defined seed mask in the anterior corpus callosum were reconstructed. Group- and tract-specific
231 connectivity distributions were finally analyzed applying different thresholds, 0.01%, 0.5%, 1.0%
232 and 2%, of the overall successful streamlines as described elsewhere (Schulz et al., 2015).

233 **2.9 Further Statistical Analyses**

234 Further statistical analyzes were performed using Matlab version 9.1 (R2016b, MathWorks,
235 Natick, MA) and R statistical package Version 3.5.4 (<http://www.r-project.org/>).
236 To test for assessment related group-differences a linear model was defined by means of R's *lm*
237 command to investigate the relationship between the assessment variables Age, MDT, 2-point-

238 discrimination, MMSE, DemTect, FEDA-A, FEDA-B, FEDA-C as dependent variables and
239 GROUP (Young, O-HP, O-LP) as independent variable. Age was included into the model to test
240 for age differences in the groups O-HP and O-LP. The comparison was performed using *lsmeans*
241 (R-package: *lsmeans*) and pairwise comparison between the resulting contrasts. Benjamini-
242 Yekutieli adaptive FDR-correction (BY) was used to adjust for multiple comparisons (Benjamini
243 and Yekutieli, 2001). For post-hoc testing a MANOVA was used with GROUP as independent
244 variable and BY correction to adjust for multiple comparisons. Task performance of groups Young
245 and O-HP was compared at each step of the recognition task with a two-sided t-test and BY
246 correction for multiple comparison.

247 Mean FA-values in anterior and posterior corpus callosum were compared between O-HP and O-
248 LP using a two-sided unpaired t-test. For the comparison of AD and RD in the anterior and
249 posterior corpus callosum between the two groups O-HP and O-LP a two-sided unpaired t-test was
250 used likewise.

251 Furthermore, linear regression models were fitted to test for relationships between diffusion
252 parameters (FA, AD and RD) and assessment parameters. Group differences were calculated by
253 means of $(diffusion\ parameter)*GROUP$. FDR-correction was performed to correct for multiple
254 comparisons.

255 **3 Results**

256 **3.1 Behavior**

257 At all steps of the tactile recognition task, younger participants (= Young, Y) performed better
258 than older participants ($p < 0.001$ at all steps). Besides this expected performance differences
259 between younger and older participants, there were also differences in the accuracy of tactile
260 pattern recognition within the older group. In the older group, 19 of 29 participants were able to
261 reach the predefined accuracy level at all steps. On each step of the tactile recognition task, some
262 older participants failed to reach the predefined target. 5 older participants were not able to detect
263 the familiarization patterns with the targeted accuracy. 3 older participants failed to detect the
264 target patterns at a stimulation time of 800ms. 2 more older participants failed to detect the target
265 patterns at a stimulation time of 500ms. These participants were then excluded from the further
266 steps. Older participants were regrouped according to their performance in O-HP (older-high-
267 performers) and O-LP (older-low-performers). Taking only the O-HP, the younger participants
268 still performed significantly better at each step (see table 1, $p < 0.001$ at all steps).

269

270

- Table 1 here -

271

272 **3.2 Assessment**

273 As the factor age was included into the model, group comparison of baseline data obtained in the
274 assessment prior to inclusion (see table 2) naturally showed significant differences between Young
275 and O-HP ($t(46) = 37.8$, $p < 0.001$) and Young and O-LP ($t(46) = 32.2$, $p < 0.001$). Importantly,
276 there was no difference between O-HP and O-LP ($t(46) = -0.93$, $p = 0.6550$). Despite their

277 differences in performance in the tactile recognition task, there were no significant differences
278 between O-HP and O-LP in the baseline data.

279 Post-hoc comparison of baseline data of Young and O-HP, showed that besides age ($F(1, 37) =$
280 $1768.1, p < 0.001$) DemTect ($F(1, 37) = 22.2, p < 0.001$) differed significantly between groups.
281 Young and O-LP differed, besides age ($F(1, 28) = 1827.6, p < 0.001$), in MDT ($F(1, 28) = 18.7, p$
282 $= 0.0019$), but not in DemTect ($F(1, 28) = 4.7, p = 0.1401$). Importantly, neither of the
283 measurements revealed pathological results in the older participants. All comparisons were
284 corrected for multiple comparison.

285

286 - Table 2 here -

287

288 **3.3 TBSS**

289 **3.3.1 Young vs O-HP and Young vs O-LP**

290 Whole brain TBSS-analysis showed significantly higher FA-values for almost every region within
291 the FA-skeleton for the younger participants compared with O-HP and O-LP (see figure 2). No
292 region showed higher FA-values for O-HP or O-LP compared with Young.

293 **3.3.2 O-HP vs. O-LP**

294 Whole brain TBSS-analysis with testing for differences between the O-HP and O-LP showed
295 significantly higher FA-values for O-HP mainly in a region in the anterior part of the corpus
296 callosum and a small region in the right anterior white matter connected to the corpus callosum.
297 This part is equivalent to the overlap between genu and body of the corpus callosum (see figure
298 2C). The mean FA-value of this anterior region showed a significant difference between O-HP and
299 O-LP ($p < 0.001$). Mean FA-values for O-HP (0.65 ± 0.02) and O-LP (0.58 ± 0.05) are additionally

300 plotted in figure 3A. In comparison, an equivalent region in the splenium corpus callosum showed
301 no significant difference between both groups (see suppl. figure 2).

302

303 - Figure 2 here -

304

305 Whole brain TBSS-analysis for AD and RD showed no significant difference between both older
306 groups within the ROI in the anterior corpus callosum. To further explore the underlying
307 microstructural alterations in the anterior corpus callosum as defined by the TBSS-FA, we opted
308 to investigate this region in detail. As illustrated by figure 3B and C analysis of AD showed
309 significantly lower values for O-LP (0.00132 ± 0.00004) compared to O-HP (0.00137 ± 0.00003 ,
310 $p = 0.001$), whereas RD was significantly higher in the group of O-LP (0.00045 ± 0.00006)
311 compared to O-HP (0.00038 ± 0.00003 , $p < 0.001$)

312

313 - Figure 3 here -

314

315 **3.4 Tractography**

316 To further explore the relevance of the TBSS results, we used probabilistic tractography to
317 reconstruct the tracts originating from the region in the anterior corpus callosum. In each
318 participant, tracts starting from the defined seed mask in the anterior corpus callosum were
319 reconstructed.

320 As indicated by figure 4, there was a substantial spatial overlay of the trajectory maps for the
321 resulting tracts for O-HP and O-LP. For each threshold, the merged tracts of all participants,
322 thresholded by 50% of all participants of each group (O-HP and O-LP), were plotted. The

323 reconstructed tracts showed ~~strong~~ connections between the seed-roi and the frontal lobe in both
324 hemispheres, comprising the bilateral frontal pole, the superior frontal, inferior frontal and middle
325 frontal gyrus, areas which are part of the prefrontal cortex. Furthermore, there were relevant
326 connections to subcortical structures such as the bilateral thalamus and the basal ganglia. Visual
327 inspection did not show group differences in the connected regions.

328

329

- Figure 4 here -

330

331 **4 Discussion**

332 This study aimed to explore complex sensory processing in younger and healthy older participants
333 and to test the hypothesis that white matter structure has an impact on tactile behavioral
334 performance. The data showed that, over all, older participants performed worse in a complex
335 tactile recognition task. Intriguingly, a subgroup of the older participants showed particular low
336 performance (O-LP), in contrast to another better performing older subgroup (O-HP). Diffusion-
337 weighted imaging helped to better understand this bimodal distribution. The main finding was a
338 significantly reduced microstructural integrity of transcallosal fibers, particularly in the anterior
339 corpus callosum, in O-LP compared to O-HP. This performance-related alteration of brain
340 structure might serve as a surrogate marker for early structural network alteration leading to
341 differences in central processing and ultimately performance.

342
343 A decrease of FA with increasing age has been reported in multiple previous studies (Abe et al.,
344 2002; Kochunov et al., 2007; Moseley, 2002). During aging, FA in genu and body of the corpus
345 callosum has been shown to decrease earlier than in other regions (e.g. splenium corpus callosi)
346 (Bennett et al., 2010; Burzynska et al., 2010; Kochunov et al., 2012; Madden et al., 2007, 2004;
347 Michielse et al., 2010; Pfefferbaum et al., 2000; Sullivan et al., 2001). In the present data, O-HP
348 and O-LP only differed in the FA in this area. In the context of alternative diffusion metrics, that
349 were reduced AD and increased RD, the reduction of white-matter integrity of transcallosal fibers
350 could be a result of age-dependent alterations both in myelinisation and axonal integrity
351 (Alexander et al., 2011; Feldman et al., 2010).

352 The potential meaning of this reduced microstructural integrity in the anterior corpus callosum as
353 a marker for early structural network alterations might be supported by its neuroanatomical

354 properties. It has been shown that the anterior part of the corpus callosum mainly contains thinly
355 myelinated, densely packed fibers that connect pre-frontal brain areas (Kochunov et al., 2007).
356 These fibers mature later and exhibit earlier deterioration during aging than the more thickly
357 myelinated fibers in the body and splenium of the corpus callosum connecting motor or sensory
358 areas (Bartzokis, 2004; Brickman et al., 2012; Kochunov et al., 2007). It has been hypothesized
359 that the oligodendrocytes that myelinate the tracts passing the anterior corpus callosum are among
360 the most metabolically active cells in the adult nervous system. This would make these cells
361 susceptible to accumulation of metabolic damage and proposes a potential hypothesis on why the
362 anterior corpus callosum might be more vulnerable to aging processes than other brain regions
363 (Bartzokis, 2004; Kochunov et al., 2007). This hypothesis might provide a pathophysiological
364 basis for our results and might indicate that reduced microstructural integrity could be caused by
365 specific properties of the fiber system passing the anterior corpus callosum (Bennett and Madden,
366 2014; Salat, 2011; Salat et al., 2005).

367

368 The anterior corpus callosum has been shown to mainly connect pre-frontal brain areas (Kochunov
369 et al., 2007) We used probabilistic tractography to further relate the local FA reduction in the
370 anterior corpus callosum in O-LP to the underlying structural networks.

371 Information flow between distant brain regions has been shown to be of critical importance for
372 processing of sensory information (Ni and Chen, 2017). As discussed in the introduction, sensory
373 processing relies on distributed networks relevant for bottom-up sensory flow and top-down
374 control. Alterations in both might lead to disturbances in tactile recognition. Hence, the
375 identification of specific neuronal networks affected by the decrease in microstructural white

376 matter integrity might give insights into the reasons for poor task performance in O-LP (Coxon et
377 al., 2012).

378

379 Probabilistic tractography showed strong connections from the anterior corpus callosum to the
380 frontal pole, the inferior, middle and superior frontal gyrus, heterogeneous brain regions
381 contributing to prefrontal cortices (PFC), such as the dorsolateral (DFPLC) and ventrolateral
382 (VLPFC) prefrontal cortex and also the orbitofrontal cortex (OFC). The PFC has been shown to
383 be relevant for various higher-order cognitive processes, e.g. working memory (Funahashi, 2017;
384 Miller et al., 2002; Miller and Cohen, 2001). More specifically, the DFPLC is known for its role
385 in the executive functions, such as selective attention and cognitive flexibility (Curtis and
386 D'Esposito, 2003; Gläscher et al., 2012; Kim et al., 2011). The VLPFC has been reported to be an
387 important node in elaborate attentional processes and top-down processing of sensory information
388 (Tops and Boksem, 2011; Uno et al., 2015). The OFC is involved in decision making (Fellows,
389 2007; Wallis, 2007). In addition to possible connections between these cortical brain regions,
390 higher cognitive processes are also reliant on cortico-subcortical circuits, connecting cortical brain
391 areas with the thalamus (Behrens et al., 2003; Ferguson and Gao, 2015) and the basal ganglia
392 (McNab and Klingberg, 2008; Voytek and Knight, 2010). Well in line with this, the identified
393 region in the anterior corpus callosum was also found to be connected bilaterally to the thalamus
394 and the basal ganglia.

395 Taken together, probabilistic tractography confirmed that the identified region in the anterior
396 corpus callosum mainly connects pre-frontal cortices. The reduction of microstructural integrity in
397 the anterior corpus callosum might lead to functional disturbances in these frontal cortico-cortical
398 and cortico-subcortical networks and impede cognitive processes related to attention and working-

399 memory which are important for complex sensory information. Linking the structural finding to
400 the behavioral results, one could argue that the disturbance of the identified networks might be a
401 possible reason for poor task performance in O-LP. Interestingly, there were no relevant structural
402 connectivity between the seed region and parietal brain areas, suggesting that poor performance of
403 O-LP seems not to be primarily related to networks relevant for primary central stimulus
404 processing.

405

406 In order to exclude potential confounding factors, we also investigated alternative reasons for the
407 group difference between O-HP and O-LP. First, there was no age difference between O-HP and
408 O-LP. Second, there was no difference in peripheral somatosensation between the two groups. In
409 contrast, behavioral tests comparing younger and older individuals pointed to a difference in the
410 MDT which tended to be worse in the older participants. Of note, this difference became only
411 significant when comparing Young selectively to O-LP. Third, there was no difference in the
412 neurophysiological assessment between O-HP and O-LP. O-LP even had higher scores in
413 DemTect and did not differ significantly from Young. While all participants with pathological test
414 results were excluded, there still was a significant difference between Young and O-HP in
415 DemTect.

416 Taken together, possible reasons of performance differences between younger and older
417 participants are manifold, comprising differences in peripheral stimuli processing, cognitive
418 decline, but also structural changes of the brain. Comparing O-HP and O-LP, the only difference
419 was found in brain imaging and the regional microstructure in the anterior corpus callosum. We
420 argue that this might be a specific finding showing a progressed aging of the brain and explaining
421 performance differences.

422

423 On a speculative note, biological age might not and neurophysiological assessment might not yet
424 reflect the progressed aging of the brain in O-LP. The complex tactile recognition task might be a
425 sensitive marker for a more general early cognitive impairment, potentially more sensitive than
426 common neurophysiological measures. As one of the most important endeavors in this field is to
427 identify individuals suffering from age-related impairments to allow for early support and
428 interventions, complex tactile recognition might be one asset. Still, due to the found alterations in
429 networks relevant for higher order cognitive processes, early cognitive impairment might also be
430 assessed by complex sensory tasks in other modalities, which rely on the same frontal networks
431 connected by the anterior corpus callosum.

432

433 There are some limitations to the current study. Due to group allocation based on performance,
434 sample size of O-HP and O-LP differed which might limit statistical robustness of the results.
435 Additionally, overall sample sizes were small and this might question the generalizability of the
436 present results. Especially for any negative results we cannot preclude that a larger sample size
437 would detect smaller effects. This is why we did not report any small effects but restricted our
438 analyzes and interpretation to the very large effect found in the anterior corpus callosum. Though,
439 the current study might help to generate hypotheses for further explorations. For instance,
440 prospective studies would help to investigate structural integrity in the anterior corpus callosum
441 over time. Likewise, the effects of behavioral training on FA in this region could be evaluated by
442 future longitudinal studies, which thereby might also infer causality of the present findings.

443

444 In conclusion, the only difference found between healthy older low- and high performers in a
445 complex tactile recognition task was a decreased microstructural white-matter integrity in the

446 anterior corpus callosum. In line with the literature, showing that due to it's neuroanatomical
447 properties the anterior corpus callosum is most vulnerable to aging processes, we argue that this
448 might be a specific finding showing a progressed aging of the brain and explaining performance
449 differences. Sensory processing relies on both, primary sensory processing and higher cognitive
450 processes. As the vulnerable region in the anterior corpus callosum mainly connects pre-frontal
451 cortices, our results suggest that disturbances in higher order cognitive processes are the reason
452 for early decline with aging.

453 **Declarations of interest:** None

454 **Funding:** This work was supported by the German Research Foundation (DFG) and the National

455 Science Foundation of China (NSFC) in project Crossmodal Learning, TRR-169/A3

456 **5 References**

- 457 Abe O, Aoki S, Hayashi N, Yamada H, Kunimatsu A, Mori H, et al. Normal aging in the central
458 nervous system: quantitative MR diffusion-tensor analysis. *Neurobiol Aging* 2002;23:433–
459 41.
- 460 Adhikari BM, Sathian K, Epstein CM, Lamichhane B, Dhamala M. Oscillatory Activity in
461 Neocortical Networks during Tactile Discrimination near the Limit of Spatial Acuity.
462 *Neuroimage* 2014;91:300–10. doi:10.1016/j.neuroimage.2014.01.007.
- 463 Alexander AL, Hurley SA, Samsonov AA, Adluru N, Hosseinbor AP, Mossahebi P, et al.
464 Characterization of Cerebral White Matter Properties Using Quantitative Magnetic
465 Resonance Imaging Stains. *Brain Connectivity* 2011;1:423–46.
466 doi:10.1089/brain.2011.0071.
- 467 Andersson JLR, Jenkinson M, Smith SM. Non-linear Registration aka Spatial Normalisation.
468 FMRIB Technical Report TR07JA2. 2007a.
- 469 Andersson JLR, Jenkinson M, Smith SM. Non-linear optimization. FMRIB Technical Report
470 TR07JA1. 2007b.
- 471 Anguera JA, Gazzaley A. Dissociation of motor and sensory inhibition processes in normal aging.
472 *Clin Neurophysiol* 2012;123:730–40. doi:10.1016/j.clinph.2011.08.024.
- 473 Babaeeghazvini P, Rueda-Delgado L, Zivari Adab H, Gooijers J, Swinnen S, Daffertshofer A. A
474 combined diffusion-weighted and electroencephalography study on age-related differences
475 in connectivity in the motor network during bimanual performance. *Human Brain Mapping*
476 2018. doi:10.1002/hbm.24491.
- 477 Bartzokis G. Age-related myelin breakdown: a developmental model of cognitive decline and
478 Alzheimer’s disease. *Neurobiol Aging* 2004;25:5–18; author reply 49-62.

- 479 Behrens TEJ, Berg HJ, Jbabdi S, Rushworth MFS, Woolrich MW. Probabilistic diffusion
480 tractography with multiple fibre orientations: What can we gain? *Neuroimage* 2007;34:144–
481 55. doi:10.1016/j.neuroimage.2006.09.018.
- 482 Behrens TEJ, Johansen-Berg H, Woolrich MW, Smith SM, Wheeler-Kingshott C a. M, Boulby
483 PA, et al. Non-invasive mapping of connections between human thalamus and cortex using
484 diffusion imaging. *Nat Neurosci* 2003;6:750–7. doi:10.1038/nn1075.
- 485 Benjamini Y, Yekutieli D. The Control of the False Discovery Rate in Multiple Testing under
486 Dependency. *The Annals of Statistics* 2001;29:1165–88.
- 487 Bennett IJ, Madden DJ. Disconnected aging: cerebral white matter integrity and age-related
488 differences in cognition. *Neuroscience* 2014;276:187–205.
489 doi:10.1016/j.neuroscience.2013.11.026.
- 490 Bennett IJ, Madden DJ, Vaidya CJ, Howard DV, Howard JH. Age-related differences in multiple
491 measures of white matter integrity: A diffusion tensor imaging study of healthy aging.
492 *Hum Brain Mapp* 2010;31:378–90. doi:10.1002/hbm.20872.
- 493 Brickman AM, Meier IB, Korgaonkar MS, Provenzano FA, Grieve SM, Siedlecki KL, et al.
494 Testing the white matter retrogenesis hypothesis of cognitive aging. *Neurobiol Aging*
495 2012;33:1699–715. doi:10.1016/j.neurobiolaging.2011.06.001.
- 496 Burzynska AZ, Preuschhof C, Bäckman L, Nyberg L, Li S-C, Lindenberger U, et al. Age-related
497 differences in white matter microstructure: region-specific patterns of diffusivity.
498 *Neuroimage* 2010;49:2104–12. doi:10.1016/j.neuroimage.2009.09.041.
- 499 Carmichael O, Lockhart S. The role of diffusion tensor imaging in the study of cognitive aging.
500 *Curr Top Behav Neurosci* 2012;11:289–320. doi:10.1007/7854_2011_176.
- 501 Chalavi S, Zivari Adab H, Pauwels L, Beets I, Ruitenbeek P, Boisgontier M, et al. Anatomy of

- 502 Subcortical Structures Predicts Age-Related Differences in Skill Acquisition. *Cerebral*
503 *Cortex* 2018;28:459–473. doi:10.1093/cercor/bhw382.
- 504 Coxon JP, Van Impe A, Wenderoth N, Swinnen SP. Aging and inhibitory control of action:
505 cortico-subthalamic connection strength predicts stopping performance. *J Neurosci*
506 2012;32:8401–12. doi:10.1523/JNEUROSCI.6360-11.2012.
- 507 Crosby PM, Dellon AL. Comparison of two-point discrimination testing devices. *Microsurgery*
508 1989;10:134–7.
- 509 Curtis CE, D’Esposito M. Persistent activity in the prefrontal cortex during working memory.
510 *Trends Cogn Sci (Regul Ed)* 2003;7:415–23.
- 511 Damoiseaux JS. Effects of aging on functional and structural brain connectivity. *NeuroImage*
512 2017;160:32–40. doi:10.1016/j.neuroimage.2017.01.077.
- 513 Deibert E, Kraut M, Kremen S, Hart J. Neural pathways in tactile object recognition. *Neurology*
514 1999;52:1413–7. doi:10.1212/wnl.52.7.1413.
- 515 Dellon ES, Keller K, Moratz V, Dellon AL. The relationships between skin hardness, pressure
516 perception and two-point discrimination in the fingertip. *J Hand Surg Br* 1995;20:44–8.
- 517 Feldman HM, Yeatman JD, Lee ES, Barde LHF, Gaman-Bean S. Diffusion Tensor Imaging: A
518 Review for Pediatric Researchers and Clinicians. *J Dev Behav Pediatr* 2010;31:346–56.
519 doi:10.1097/DBP.0b013e3181dcaa8b.
- 520 Fellows LK. The role of orbitofrontal cortex in decision making: a component process account.
521 *Ann N Y Acad Sci* 2007;1121:421–30. doi:10.1196/annals.1401.023.
- 522 Ferguson BR, Gao W-J. Development of thalamocortical connections between the mediodorsal
523 thalamus and the prefrontal cortex and its implication in cognition. *Front Hum Neurosci*
524 2015;8. doi:10.3389/fnhum.2014.01027.

- 525 Folstein MF, Folstein SE, McHugh PR. “Mini-mental state”. A practical method for grading the
526 cognitive state of patients for the clinician. *J Psychiatr Res* 1975;12:189–98.
- 527 Freiherr J, Lundström JN, Habel U, Reetz K. Multisensory integration mechanisms during aging.
528 *Front Hum Neurosci* 2013;7:863. doi:10.3389/fnhum.2013.00863.
- 529 Fruhstorfer H, Gross W, Selbmann O. von Frey hairs: new materials for a new design. *Eur J Pain*
530 2001;5:341–2. doi:10.1053/eujp.2001.0250.
- 531 Funahashi S. Working Memory in the Prefrontal Cortex. *Brain Sci* 2017;7.
532 doi:10.3390/brainsci7050049.
- 533 Gazzaley A, Cooney JW, Rissman J, D’Esposito M. Top-down suppression deficit underlies
534 working memory impairment in normal aging. *Nat Neurosci* 2005;8:1298–300.
535 doi:10.1038/nn1543.
- 536 Gläscher J, Adolphs R, Damasio H, Bechara A, Rudrauf D, Calamia M, et al. Lesion mapping of
537 cognitive control and value-based decision making in the prefrontal cortex. *PNAS*
538 2012;109:14681–6. doi:10.1073/pnas.1206608109.
- 539 Göschl F, Frieze U, Daume J, König P, Engel AK. Oscillatory signatures of crossmodal
540 congruence effects: An EEG investigation employing a visuotactile pattern matching
541 paradigm. *Neuroimage* 2015;116:177–86. doi:10.1016/j.neuroimage.2015.03.067.
- 542 Guerreiro MJS, Anguera JA, Mishra J, Van Gerven PWM, Gazzaley A. Age-equivalent top-down
543 modulation during cross-modal selective attention. *J Cogn Neurosci* 2014;26:2827–39.
544 doi:10.1162/jocn_a_00685.
- 545 Heise K-F, Niehoff M, Feldheim J-F, Liuzzi G, Gerloff C, Hummel FC. Differential behavioral
546 and physiological effects of anodal transcranial direct current stimulation in healthy adults
547 of younger and older age. *Front Aging Neurosci* 2014;6:146. doi:10.3389/fnagi.2014.00146.

- 548 Heise K-F, Zimmerman M, Hoppe J, Gerloff C, Wegscheider K, Hummel FC. The aging motor
549 system as a model for plastic changes of GABA-mediated intracortical inhibition and their
550 behavioral relevance. *J Neurosci* 2013;33:9039–49. doi:10.1523/JNEUROSCI.4094-
551 12.2013.
- 552 Heuninckx S, Wenderoth N, Swinnen SP. Systems neuroplasticity in the aging brain: recruiting
553 additional neural resources for successful motor performance in elderly persons. *J Neurosci*
554 2008;28:91–9. doi:10.1523/JNEUROSCI.3300-07.2008.
- 555 Hipp JF, Engel AK, Siegel M. Oscillatory synchronization in large-scale cortical networks predicts
556 perception. *Neuron* 2011;69:387–96. doi:10.1016/j.neuron.2010.12.027.
- 557 Hong SL, Rebec GV. A new perspective on behavioral inconsistency and neural noise in aging:
558 compensatory speeding of neural communication. *Front Aging Neurosci* 2012;4.
559 doi:10.3389/fnagi.2012.00027.
- 560 Hugenschmidt CE, Peiffer AM, Kraft RA, Casanova R, Deibler AR, Burdette JH, et al. Relating
561 imaging indices of white matter integrity and volume in healthy older adults. *Cereb Cortex*
562 2008;18:433–42. doi:10.1093/cercor/bhm080.
- 563 Kalbe E, Kessler J, Calabrese P, Smith R, Passmore AP, Brand M, et al. DemTect: a new, sensitive
564 cognitive screening test to support the diagnosis of mild cognitive impairment and early
565 dementia. *Int J Geriatr Psychiatry* 2004;19:136–43. doi:10.1002/gps.1042.
- 566 Kim C, Johnson NF, Cilles SE, Gold BT. Common and Distinct Mechanisms of Cognitive
567 Flexibility in Prefrontal Cortex. *J Neurosci* 2011;31:4771–9.
568 doi:10.1523/JNEUROSCI.5923-10.2011.
- 569 Kochunov P, Thompson PM, Lancaster JL, Bartzokis G, Smith S, Coyle T, et al. Relationship
570 between white matter fractional anisotropy and other indices of cerebral health in normal

- 571 aging: tract-based spatial statistics study of aging. *Neuroimage* 2007;35:478–87.
572 doi:10.1016/j.neuroimage.2006.12.021.
- 573 Kochunov P, Williamson DE, Lancaster J, Fox P, Cornell J, Blangero J, et al. Fractional anisotropy
574 of water diffusion in cerebral white matter across the lifespan. *Neurobiol Aging* 2012;33:9–
575 20. doi:10.1016/j.neurobiolaging.2010.01.014.
- 576 Kumar A, Foster TC. Neurophysiology of Old Neurons and Synapses. In: Riddle DR, editor. *Brain*
577 *Aging: Models, Methods, and Mechanisms*, Boca Raton (FL): CRC Press/Taylor & Francis;
578 2007.
- 579 Madden DJ, Bennett IJ, Burzynska A, Potter GG, Chen N-K, Song AW. Diffusion tensor
580 imaging of cerebral white matter integrity in cognitive aging. *Biochim Biophys Acta*
581 2012;1822:386–400. doi:10.1016/j.bbadis.2011.08.003.
- 582 Madden DJ, Bennett IJ, Song AW. Cerebral white matter integrity and cognitive aging:
583 contributions from diffusion tensor imaging. *Neuropsychol Rev* 2009;19:415–35.
584 doi:10.1007/s11065-009-9113-2.
- 585 Madden DJ, Spaniol J, Whiting WL, Bucur B, Provenzale JM, Cabeza R, et al. Adult age
586 differences in the functional neuroanatomy of visual attention: a combined fMRI and DTI
587 study. *Neurobiol Aging* 2007;28:459–76. doi:10.1016/j.neurobiolaging.2006.01.005.
- 588 Madden DJ, Whiting WL, Huettel SA, White LE, MacFall JR, Provenzale JM. Diffusion tensor
589 imaging of adult age differences in cerebral white matter: relation to response time.
590 *Neuroimage* 2004;21:1174–81. doi:10.1016/j.neuroimage.2003.11.004.
- 591 Malloy P, Correia S, Stebbins G, Laidlaw DH. Neuroimaging of white matter in aging and
592 dementia. *Clin Neuropsychol* 2007;21:73–109. doi:10.1080/13854040500263583.
- 593 Mauguière F, Merlet I, Forss N, Vanni S, Jousmäki V, Adeleine P, et al. Activation of a

- 594 distributed somatosensory cortical network in the human brain. A dipole modelling study
595 of magnetic fields evoked by median nerve stimulation. Part I: Location and activation
596 timing of SEF sources. *Electroencephalogr Clin Neurophysiol* 1997;104:281–9.
- 597 McNab F, Klingberg T. Prefrontal cortex and basal ganglia control access to working memory.
598 *Nat Neurosci* 2008;11:103–7. doi:10.1038/nn2024.
- 599 Michely J, Volz LJ, Hoffstaedter F, Tittgemeyer M, Eickhoff SB, Fink GR, et al. Network
600 connectivity of motor control in the ageing brain. *Neuroimage Clin* 2018;18:443–55.
601 doi:10.1016/j.nicl.2018.02.001.
- 602 Michielse S, Coupland N, Camicioli R, Carter R, Seres P, Sabino J, et al. Selective effects of
603 aging on brain white matter microstructure: a diffusion tensor imaging tractography study.
604 *Neuroimage* 2010;52:1190–201. doi:10.1016/j.neuroimage.2010.05.019.
- 605 Miller EK, Cohen JD. An integrative theory of prefrontal cortex function. *Annu Rev Neurosci*
606 2001;24:167–202. doi:10.1146/annurev.neuro.24.1.167.
- 607 Miller EK, Freedman DJ, Wallis JD. The prefrontal cortex: categories, concepts and cognition.
608 *Philos Trans R Soc Lond B Biol Sci* 2002;357:1123–36. doi:10.1098/rstb.2002.1099.
- 609 Minati L, Grisoli M, Bruzzone MG. MR spectroscopy, functional MRI, and diffusion-tensor
610 imaging in the aging brain: a conceptual review. *J Geriatr Psychiatry Neurol* 2007;20:3–21.
611 doi:10.1177/0891988706297089.
- 612 Moseley M. Diffusion tensor imaging and aging - a review. *NMR Biomed* 2002;15:553–60.
613 doi:10.1002/nbm.785.
- 614 Ni J, Chen JL. Long-range cortical dynamics: a perspective from the mouse sensorimotor whisker
615 system. *European Journal of Neuroscience* 2017;46:2315–24. doi:10.1111/ejn.13698.
- 616 Oldfield RC. The assessment and analysis of handedness: the Edinburgh inventory.

- 617 Neuropsychologia 1971;9:97–113.
- 618 Pfefferbaum A, Sullivan EV, Hedehus M, Lim KO, Adalsteinsson E, Moseley M. Age-related
619 decline in brain white matter anisotropy measured with spatially corrected echo-planar
620 diffusion tensor imaging. *Magn Reson Med* 2000;44:259–68.
- 621 Quandt F, Bönstrup M, Schulz R, Timmermann JE, Zimmerman M, Nolte G, et al. Spectral
622 Variability in the Aged Brain during Fine Motor Control. *Front Aging Neurosci* 2016;8.
623 doi:10.3389/fnagi.2016.00305.
- 624 Raz N, Rodrigue KM. Differential aging of the brain: patterns, cognitive correlates and modifiers.
625 *Neurosci Biobehav Rev* 2006;30:730–48. doi:10.1016/j.neubiorev.2006.07.001.
- 626 Reed CL, Shoham S, Halgren E. Neural substrates of tactile object recognition: An fMRI study.
627 *Human Brain Mapping* 2004;21:236–46. doi:10.1002/hbm.10162.
- 628 Rolke R, Magerl W, Campbell KA, Schalber C, Caspari S, Birklein F, et al. Quantitative sensory
629 testing: a comprehensive protocol for clinical trials. *Eur J Pain* 2006;10:77–88.
630 doi:10.1016/j.ejpain.2005.02.003.
- 631 Rueckert D, Sonoda LI, Hayes C, Hill DLG, Leach MO, Hawkes DJ. Nonrigid registration using
632 free-form deformations: application to breast MR images. *IEEE Trans Med Imag*
633 1999;18:712–21. doi:10.1109/42.796284.
- 634 Sailer A, Dichgans J, Gerloff C. The influence of normal aging on the cortical processing of a
635 simple motor task. *Neurology* 2000;55:979–85.
- 636 Salat DH. The declining infrastructure of the aging brain. *Brain Connect* 2011;1:279–93.
637 doi:10.1089/brain.2011.0056.
- 638 Salat DH, Tuch DS, Greve DN, van der Kouwe AJW, Hevelone ND, Zaleta AK, et al. Age-
639 related alterations in white matter microstructure measured by diffusion tensor imaging.

- 640 Neurobiol Aging 2005;26:1215–27. doi:10.1016/j.neurobiolaging.2004.09.017.
- 641 Sathian K. Analysis of haptic information in the cerebral cortex. J Neurophysiol 2016;116:1795–
642 806. doi:10.1152/jn.00546.2015.
- 643 Schulz R, Braass H, Liuzzi G, Hoerniss V, Lechner P, Gerloff C, et al. White matter integrity of
644 premotor-motor connections is associated with motor output in chronic stroke patients.
645 Neuroimage Clin 2015;7:82–6. doi:10.1016/j.nicl.2014.11.006.
- 646 Schulz R, Zimmerman M, Timmermann JE, Wessel MJ, Gerloff C, Hummel FC. White matter
647 integrity of motor connections related to training gains in healthy aging. Neurobiol Aging
648 2014;35:1404–11. doi:10.1016/j.neurobiolaging.2013.11.024.
- 649 Smith SM. Fast robust automated brain extraction. Hum Brain Mapp 2002;17:143–55.
650 doi:10.1002/hbm.10062.
- 651 Smith SM, Jenkinson M, Johansen-Berg H, Rueckert D, Nichols TE, Mackay CE, et al. Tract-
652 based spatial statistics: voxelwise analysis of multi-subject diffusion data. Neuroimage
653 2006;31:1487–505. doi:10.1016/j.neuroimage.2006.02.024.
- 654 Smith SM, Jenkinson M, Woolrich MW, Beckmann CF, Behrens TEJ, Johansen-Berg H, et al.
655 Advances in functional and structural MR image analysis and implementation as FSL.
656 Neuroimage 2004;23 Suppl 1:S208-219. doi:10.1016/j.neuroimage.2004.07.051.
- 657 Stilla R, Deshpande G, LaConte S, Hu X, Sathian K. Posteromedial parietal cortical activity and
658 inputs predict tactile spatial acuity. J Neurosci 2007;27:11091–102.
659 doi:10.1523/JNEUROSCI.1808-07.2007.
- 660 Sullivan EV, Adalsteinsson E, Hedehus M, Ju C, Moseley M, Lim KO, et al. Equivalent
661 disruption of regional white matter microstructure in ageing healthy men and women.
662 Neuroreport 2001;12:99–104. doi:10.1097/00001756-200101220-00027.

- 663 Sullivan EV, Pfefferbaum A. Neuroradiological characterization of normal adult ageing. *Br J*
664 *Radiol* 2007;80 Spec No 2:S99-108. doi:10.1259/bjr/22893432.
- 665 Sullivan EV, Pfefferbaum A. Diffusion tensor imaging and aging. *Neurosci Biobehav Rev*
666 2006;30:749–61. doi:10.1016/j.neubiorev.2006.06.002.
- 667 Tops M, Boksem MAS. A Potential Role of the Inferior Frontal Gyrus and Anterior Insula in
668 Cognitive Control, Brain Rhythms, and Event-Related Potentials. *Front Psychol* 2011;2.
669 doi:10.3389/fpsyg.2011.00330.
- 670 Uno T, Kawai K, Sakai K, Wakebe T, Ibaraki T, Kunii N, et al. Dissociated Roles of the Inferior
671 Frontal Gyrus and Superior Temporal Sulcus in Audiovisual Processing: Top-Down and
672 Bottom-Up Mismatch Detection. *PLoS One* 2015;10. doi:10.1371/journal.pone.0122580.
- 673 Van Boven RW, Ingeholm JE, Beauchamp MS, Bickle PC, Ungerleider LG. Tactile form and
674 location processing in the human brain. *Proc Natl Acad Sci U S A* 2005;102:12601–5.
675 doi:10.1073/pnas.0505907102.
- 676 Voytek B, Knight RT. Prefrontal cortex and basal ganglia contributions to visual working memory.
677 *Proc Natl Acad Sci U S A* 2010;107:18167–72. doi:10.1073/pnas.1007277107.
- 678 Wallis JD. Orbitofrontal cortex and its contribution to decision-making. *Annu Rev Neurosci*
679 2007;30:31–56. doi:10.1146/annurev.neuro.30.051606.094334.
- 680 Wozniak JR, Lim KO. Advances in white matter imaging: a review of in vivo magnetic
681 resonance methodologies and their applicability to the study of development and aging.
682 *Neurosci Biobehav Rev* 2006;30:762–74. doi:10.1016/j.neubiorev.2006.06.003.
- 683 Zheng L, Gao Z, Xiao X, Ye Z, Chen C, Xue G. Reduced Fidelity of Neural Representation
684 Underlies Episodic Memory Decline in Normal Aging. *Cereb Cortex* 2018;28:2283–96.
685 doi:10.1093/cercor/bhx130.

686 Zimmerman E, Lahav A. The multisensory brain and its ability to learn music. *Ann N Y Acad Sci*
687 2012;1252:179–84. doi:10.1111/j.1749-6632.2012.06455.x.

688 **Tables**

689 **Tab.1: Performance of the different groups.**

690

Task	Young (n=20)	O-HP (n=19)	O-LP (n=10)
Familiarization patterns for 800ms	96.9 (\pm 3.7)*	85.2 (\pm 9.7)*	47.8 (\pm 8.0) (n=5)
Target patterns for 800ms	93.1 (\pm 5.2)*	76.4 (\pm 8.9)*	54.4 (\pm 1.7) (n=3)
Target patterns for 500ms	97.7 (\pm 5.1)*	82.6 (\pm 10.7)*	54.4 (\pm 6.8) (n=2)

691

692 Mean values over all blocks needed per participant are shown in % \pm standard deviation for each

693 step of the tactile recognition task. Group comparisons between Young and O-HP were calculated

694 at each step of the recognition task with a two-sided t-test and BY correction for multiple

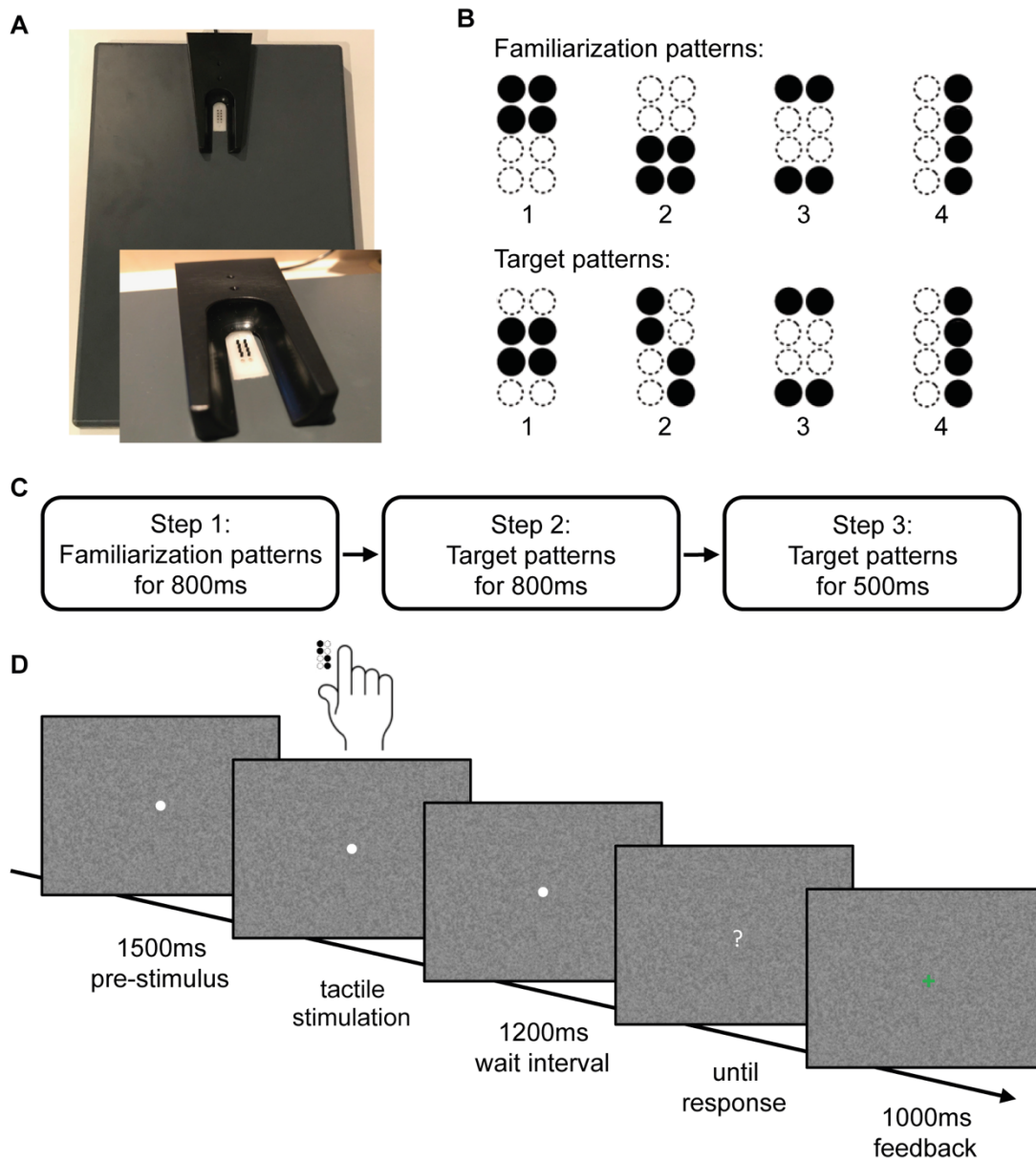
695 comparison. * indicate significant differences between Young and O-HP, all p-values \leq 0.001.

696 **Tab. 2: Assessment data of the groups.**

Metrics	Young (n=20)	O-HP (n=19)	O-LP (n=10)
Age	24.1 (\pm 2.6)* ⁺	71.9 (\pm 4.4)*	74.1 (\pm 3.9) ⁺
Height (m)	1.76(\pm 0.09)	1.69 (\pm 0.09)	1.71 (\pm 0.12)
Weight (kg)	71.3 (\pm 12.6)	68.2 (\pm 11.3)	80.8 (\pm 23.2)
BMI (kg/m ²)	22.9 (\pm 2.4)	23.8 (\pm 2.9)	27.1 (\pm 5.7)
Education (years)	12.5 (\pm 0.6)	10.7 (\pm 1.6)	11.7 (\pm 2.0)
DemTect	17.8 (\pm 0.6)*	16.0 (\pm 1.6)*	16.9 (\pm 1.6)
MMSE	29.7 (\pm 0.6)	29.5 (\pm 0.6)	29.2 (\pm 0.8)
2-Point (mm)	2.1 (\pm 0.2)	2.2 (\pm 0.4)	2.4 (\pm 0.5)
MDT (mN)	0.28 (\pm 0.1) ⁺	0.56 (\pm 0.5)	0.65 (\pm 0.4) ⁺
FEDA A	4.28 (\pm 0.4)	4.35 (\pm 0.4)	4 (\pm 0.5)
FEDA B	4.55 (\pm 0.4)	4.65 (\pm 0.4)	3.97 (\pm 0.8)
FEDA C	4.35 (\pm 0.6)	4.38 (\pm 0.5)	3.75 (\pm 0.9)

697 Mean values are shown \pm standard deviation. Based on significant main effects, post-hoc tests
698 were conducted. * indicate significant differences between Young and O-HP, ⁺ indicate significant
699 differences between Young and O-LP, all p-values \leq 0.01

700 **Figures**

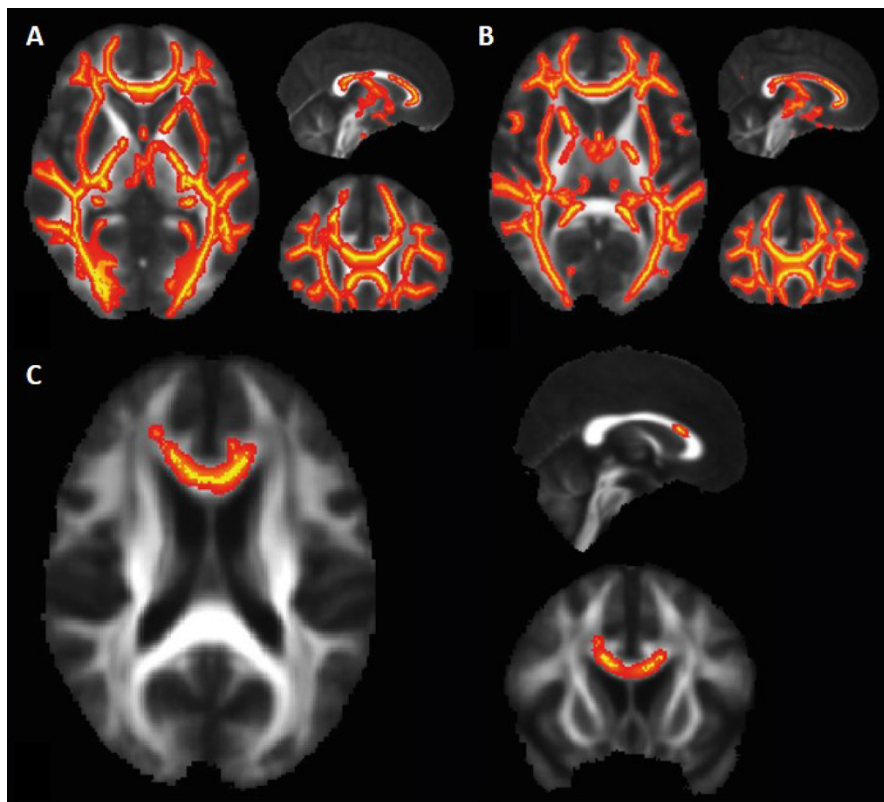


701

702 **Fig. 1: Stimulus design and experimental procedure.**

703 **A:** Braille stimulator. For tactile stimulation, the participants' right hand was resting on a custom-
704 made board containing a Braille stimulator (QuaeroSys Medical Devices, Schotten, Germany),
705 with the fingertip of the right index finger placed above the stimulating unit. The Braille stimulator
706 consists of eight pins arranged in a four-by-two matrix, each 1mm in diameter with a spacing of

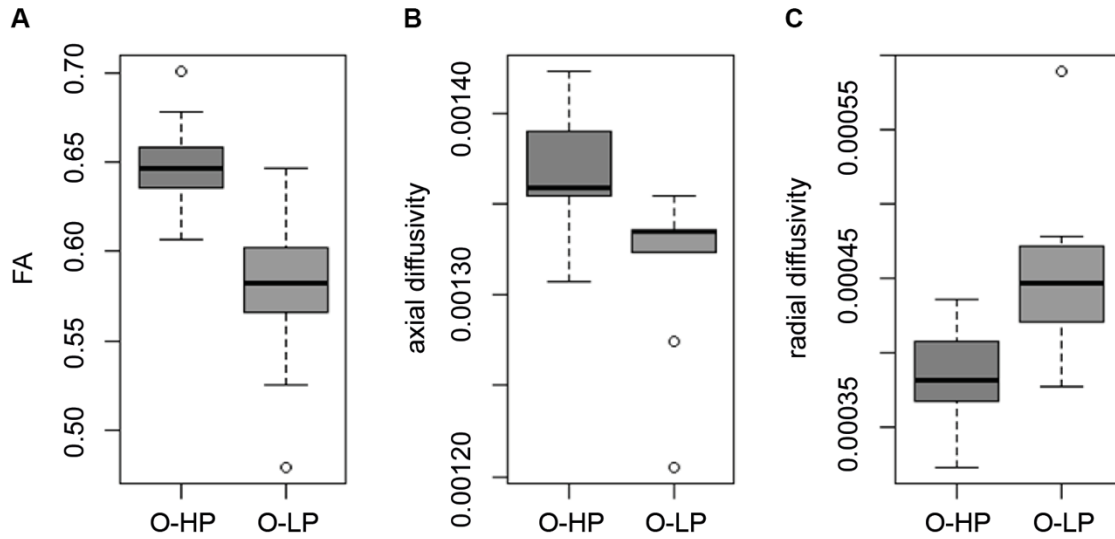
707 2.5mm. Each pin is controllable independently. **B:** Stimuli consisted of two sets of four tactile
708 patterns, **C:** Sequence of tasks in the experiment, **D:** The trial sequence. After a pre-stimulus
709 interval of 1500ms, tactile patterns were presented to the right index finger with a duration
710 depending on the current step of the experiment. After a wait interval of 1200ms, a question mark
711 appeared on the screen and participants gave the response via button press. After response, every
712 trial ended with a visual feedback (1000ms)
713



714

715 **Fig. 2: TBSS-Results, FA.**

716 **A:** $Y > O\text{-HP}$, $p < 0.05$ (red), FWE-corrected, projected on the mean-FA, MNI-coordinates
717 $(x,y,z)=(90,153,92)$, **B:** $Y > O\text{-LP}$, $p < 0.05$ (red), FWE-corrected, projected on the mean-FA, MNI-
718 coordinates $(x,y,z)=(90,155,92)$, **C:** $O\text{-HP} > O\text{-LP}$, $p < 0.05$, FWE-corrected, projected on the
719 mean-FA, MNI-coordinates $(x,y,z)=(90,141,90)$

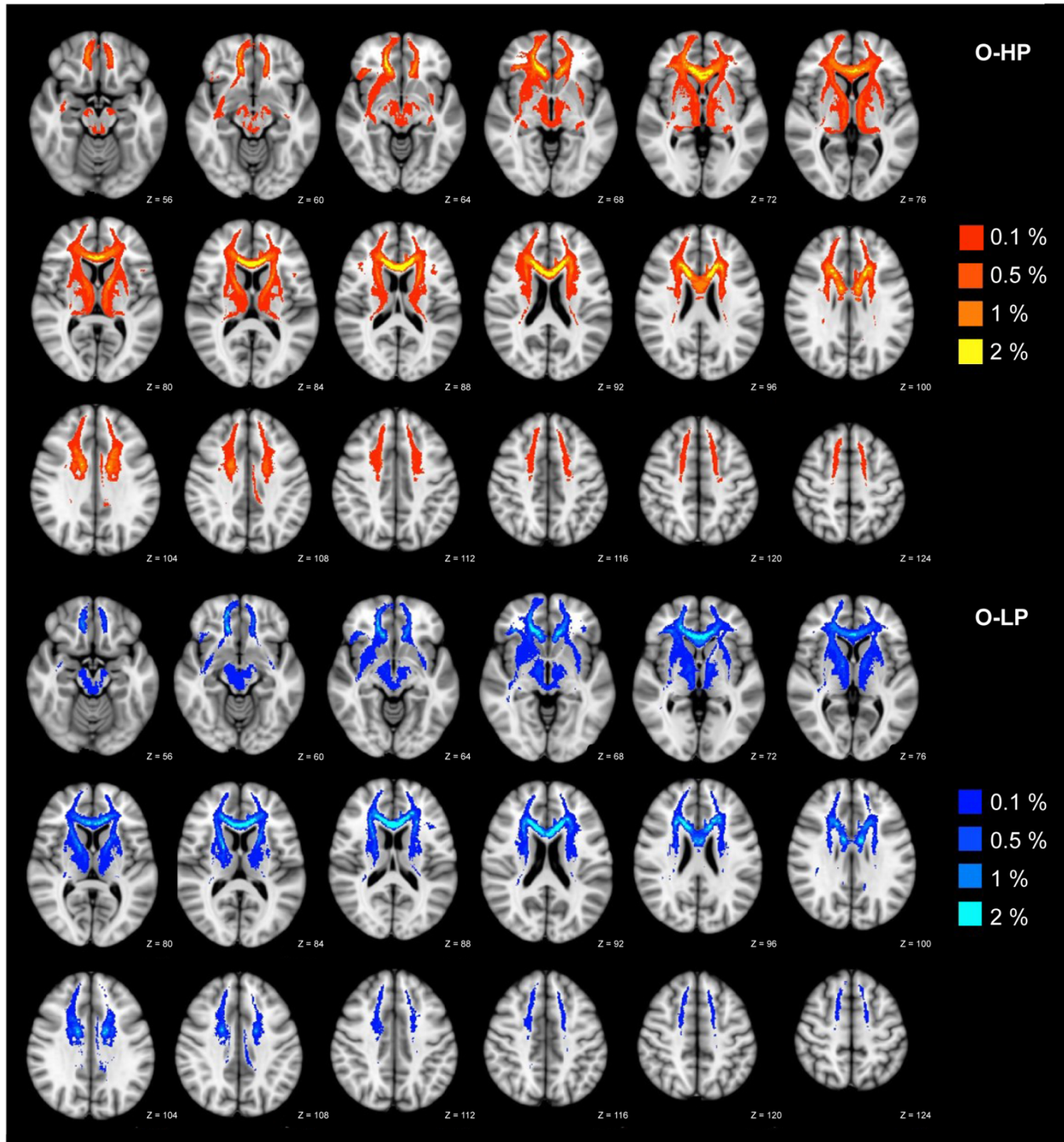


720

721 **Fig. 3: Mean FA, AD and RD for O-HP and O-LP in the anterior corpus callosum.**

722 **A:** mean FA, two-sided t-test, $p < 0.001$ (O-HP > O-LP), **B:** mean AD, two-sided t-test, $p = 0.001$ (O-

723 HP > O-LP), **C:** mean RD, two-sided t-test, $p < 0.001$ (O-LP > O-HP)



724

725 **Fig. 4: Trajectory map for the resulting tracts for O-HP and O-LP.**

726 The resulting connections are superimposed on a MNI T1 template for both groups with given z-
727 values. Overlay of binarized group average tracts, thresholded by 50% for both groups. Individual
728 tractography was conducted applying 5000 streamlines per voxel and thresholded by 0.1–2.0% of
729 successful streamlines.